Production of doubly charged vector bilepton pairs at $\gamma\gamma$ colliders

C. G. Honorato* and J. J. Toscano†

Facultad de Ciencias Físico Matemáticas, Benemérita Universidad Autónoma de Puebla,
Apartado Postal 1152, Puebla, Puebla, México

The production of pairs of doubly charged vector bileptons is studied at future $\gamma\gamma$ colliders. The unpolarized cross section for the $\gamma\gamma \to Y^{--}Y^{++}$ subprocess is analytically calculated and convoluted to predict the number of events in the complete $e^+e^- \to \gamma\gamma \to Y^{--}Y^{++}$ process. The gauge or nongauge character of the vector bilepton $Y^{\pm\pm}$ is discussed. It is found that, as a consequence of its spectacular signature, as it decays dominantly into two identical charged leptons, and also due to its charge contents, which significantly enhance the cross section, the detection of this class of particles with mass in the sub-TeV region can be at the reach of these colliders. The model-independent nature of our results is stressed.

I. INTRODUCTION

There are many reasons to believe that new physics beyond the Fermi scale must exist, but it remains unclear just how or where it will observed. However, it is quite likely that signals of new physics would be more evident in those processes which are forbidden or strongly suppressed in the standard model (SM). One possible source of new physics effects could be associated with processes that violate global conservation laws, such as, for instance, lepton number, since there is no reason to believe in its exactness. One peculiarity of the standard model (SM) is that none of its bosons carry global quantum numbers. As a consequence, lepton number is conserved both separately and globally. However, many SM extensions predict physical processes that can violate such conservation laws. For instance, the separate lepton number conservation is violated by bileptons, which are scalar or vector particles that carry two units of lepton number. This class of particles can arise in many well motivated SM extensions [1]. For instance, scalar bileptons are present in theories with enlarged Higgs sectors, as left-right symmetric models [2] in which appear doubly charged scalars coupling to pairs of identical leptons. As far as nongauge massive vectors are concerned, they are present in composite [3] and technicolor [4] theories. On the other hand, massive gauge bileptons can appear when the SM gauge group is embedded into a larger gauge group, such as occurs in the SU(15) unified model [5] or in the so-called 331 models [6], which are based in the $SU_C(3) \times SU_L(3) \times U_X(1)$ group.

In this work, we study the production of pairs of doubly charged vector bileptons $Y^{\pm\pm}$ in high-energy $\gamma\gamma$ collisions with the photons originating from Compton laser backscattering. The $\gamma\gamma \to Y^{\pm\pm}Y^{\mp\mp}$ reaction is interesting for several reasons. First, there is the distinctive signature of this class of bileptons, as they predominantly decay into two identical charged leptons, i.e. $Y^{\pm\pm} \to 2l^{\pm}$, which consti-

tutes an almost SM background-free signal. In fact, a possible source of SM background-free signal is the process $\gamma\gamma \to Z^*W^{-*}W^{+*} \to 4l^{\pm}\bar{\nu}_l\nu_l$, which evidently is very suppressed. Second, this process can be studied in a model-independent manner, since it is entirely governed by the electromagnetic $U_e(1)$ symmetry. In this respect, we will introduce the most general dimension-four $U_e(1)$-invariant Lagrangian. As already mentioned, one interesting peculiarity of a vector bilepton is the fact that it could be a gauge field (GF) or a nongauge vector field [from now on we will refer to it simply as a Proca Field (PF)], which appears reflected in the high-energy behavior of the cross section. The GF or PF nature of the vector bilepton will be incorporated in the $U_e(1)$-invariant Lagrangian and its phenomenological implications discussed. Finally, a third reason to study this process is the fact that its cross section is larger than that associated with a singly charged particle by a factor of $Q_Y^4 = 2^4 = 16$. On the other hand, the prospects for the detection of bileptons at future colliders have been extensively studied in the literature by several authors. Since bileptons couple mainly to leptons, most works have been focused on colliders involving at least one lepton beam. The potential of next linear colliders operating in the same charge mode to produce doubly charged bileptons as a s-channel resonance has received special attention [7–9]. In particular, the $e^-e^- \to Y^{--} \to \mu^-\mu^-$ process is specially suited for search of doubly charged GF, since their couplings to leptons are large and prescribed [9]. These colliders can also be used to study doubly charged scalar resonances [8], though it should be noted that in this case their couplings to leptons are free parameters and are small, as they arise from the Yukawa sector. Most studies on GF bilepton production have been done in the context of the minimal 331 model, which predicts the existence of a pair of singly and doubly charged gauge bosons, $Y_\mu^\pm$ and $Y_\mu^{\pm\pm}$ [10]. Diverse production mechanisms have been analyzed at hadron [11], e^-p [12], e^+e^- [13], $e^-\gamma$ [14], and muon [15] colliders. Though single vector bilepton production has been studied at $\gamma\gamma$ colliders [16], to our knowledge, the

---

*Electronic address: est073@fcfm.buap.mx
†Electronic address: jtoscano@fcfm.buap.mx

issue of pairs production at this type of colliders only has been tackled marginally [1]. In this paper, we will present a comprehensive study of the $\gamma\gamma \rightarrow Y^{--}Y^{++}$ process, which includes the derivation of explicit analytical expressions for the cross section of the $\gamma\gamma \rightarrow Y^{--}Y^{++}$ subprocess. In addition to dealing with both the GF and PF cases, our results will be applicable to a wide range of models, as they were derived by invoking only the general principles of renormalization theory, Lorentz invariance, and $U_e(1)$-gauge invariance.

The paper has been organized as follows. In Sec. II, the most general Lorentz and $U_e(1)$-invariant Lagrangian, which includes only interactions up to dimension four, is presented. In Sec. III, the cross section for the complete $e^+e^- \rightarrow \gamma\gamma \rightarrow Y^{\pm\pm}Y^{\mp\mp}$ reaction is derived. In Secs. IV and V, we discuss our results and present the conclusions, respectively.

II. THE $U_e(1)$-INVARIANT LAGRANGIAN AND FEYNMAN RULES

In this section, we discuss the general structure of the couplings between a doubly charged vector bilepton and the electromagnetic gauge field. The most general Lagrangian including interactions up to dimension four, which respects the Lorentz and electromagnetic symmetries, can be written as

$$\mathcal{L} = -\frac{1}{2}(D_\mu Y_\nu^{++} - D_\nu Y_\mu^{++})^\dagger(D^\mu Y^{++\nu} - D^\nu Y^{++\mu})$$
$$+ m_Y^2 Y_\mu^{--} Y^{++\mu} - ieQ_Y\kappa F_{\mu\nu}Y^{--\mu}Y^{++\nu}$$
$$-\frac{1}{4}F_{\mu\nu}F^{\mu\nu}, \tag{1}$$

where $D_\mu = \partial_\mu - ieQ_Y A_\mu$ and $F_{\mu\nu} = \partial_\mu A_\nu - \partial_\nu A_\mu$ are the covariant derivative and the field strength tensor associated with the $U_e(1)$ gauge group, respectively. In addition, $Q_Y = 2$ is the electric charge of the bilepton in units of the positron charge and κ is a dimensionless parameter, which is related with the CP-even on-shell electromagnetic properties of the $Y^{\pm\pm}$ vector field, namely, the magnetic dipole moment and the electric quadrupole moment [17]. The good high-energy behavior of the theory and therefore its renormalizability depends critically on the precise value of this parameter. The $\kappa = 0$ case corresponds to a PF, which can be present in effective field frameworks, such as technicolor theories [18]. On the other hand, GF bileptons are identified with $\kappa = 1$. In this case, the $F_{\mu\nu}Y^{--\mu}Y^{++\nu}$ term arises just from a Yang-Mills Lagrangian, such as the one associated with the 331 models [10]. The possibility of a parameter $\kappa = 1 + \Delta\kappa$, with $\Delta\kappa \ll 1$, cannot be ruled out in the case of a GF, as the $\Delta\kappa$ correction can be associated with anomalous contributions arising from radiative corrections within the context of a wider theory. This type of deviations is well-known from the SM W boson, as they have been widely studied within the context of electroweak effective Lagrangians [19]. Although all these possibilities are in principle of physical
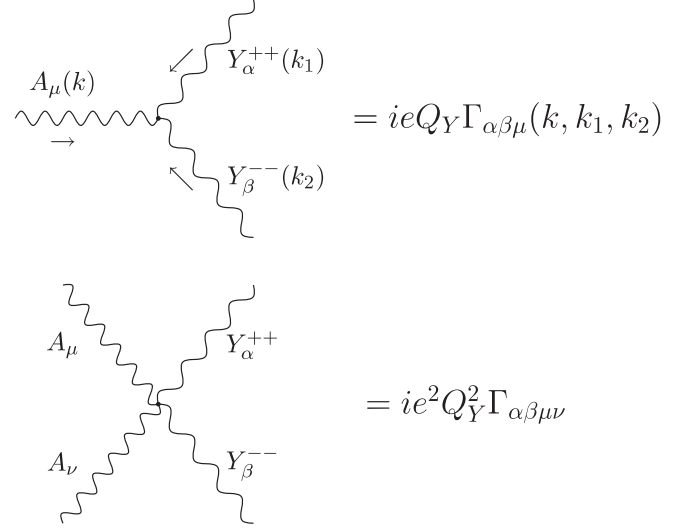

FIG. 1. Feynman rules for the $Y^{--}Y^{++}\gamma$ and $Y^{--}Y^{++}\gamma\gamma$ vertices.

interest, it is important to stress that the amplitude associated with the $\gamma\gamma \rightarrow Y^{--}Y^{++}$ scattering has a good high-energy behavior only for $\kappa = 1$ [20]. Bellow we will retain the κ parameter until we proceed with the analysis of the cross section for the complete $e^+e^- \rightarrow \gamma\gamma \rightarrow Y^{--}Y^{++}$ process.

We now turn to present the Feynman rules for the $Y^{--}Y^{++}\gamma$ and $Y^{--}Y^{++}\gamma\gamma$ vertices. Our notation and conventions are shown in Fig. 1, where the $\Gamma_{\alpha\beta\mu}(k, k_1, k_2)$ and $\Gamma_{\alpha\beta\mu\nu}$ Lorentz tensors are given by

$$\Gamma_{\alpha\beta\mu}(k, k_1, k_2) = (k_1 - k_2)_\mu g_{\alpha\beta} + (k_2 - \kappa k)_\alpha g_{\beta\mu}$$
$$- (k_1 - \kappa k)_\beta g_{\alpha\mu}, \tag{2}$$

$$\Gamma_{\alpha\beta\mu\nu} = -2g_{\alpha\beta}g_{\mu\nu} + g_{\alpha\mu}g_{\beta\nu} + g_{\alpha\nu}g_{\beta\mu}. \tag{3}$$
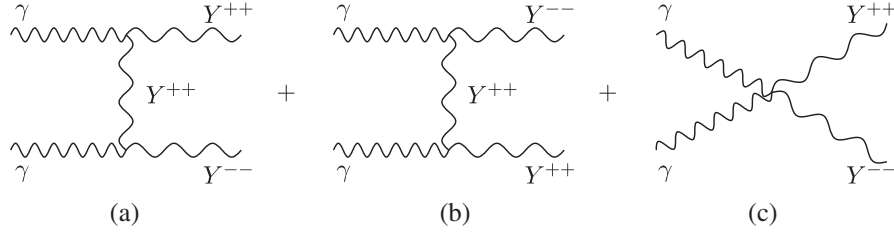
III. THE CROSS SECTION

In this section, we calculate the cross section associated with the complete $e^+e^- \rightarrow \gamma\gamma \rightarrow Y^{--}Y^{++}$ process. We first discuss the properties of the $\gamma\gamma \rightarrow Y^{--}Y^{++}$ subprocess. We will use the following notation:

$$A_\mu(k_1) + A_\nu(k_2) \rightarrow Y_\alpha^{++}(k_3) + Y_\beta^{--}(k_4), \tag{4}$$

where $k_1 + k_2 = k_3 + k_4$. With this convention, the corresponding Mandelstam variables are given by $\hat{s} = (k_1 + k_2)^2$, $\hat{t} = (k_1 - k_3)^2$, and $\hat{u} = (k_2 - k_3)^2$, which satisfy the relation $\hat{s} + \hat{t} + \hat{u} = 2m_Y^2$. In Fig. 2, we show the Feynman diagrams contributing to the invariant amplitude, which can be written as

$$\mathcal{M} = -4\pi i\alpha Q_Y^2 \mathcal{M}_{\mu\nu\alpha\beta}\epsilon^\mu(k_1, \lambda_1)\epsilon^\nu(k_2, \lambda_2)\epsilon^{\alpha*}(k_3, \lambda_3)$$
$$\times \epsilon^{\beta*}(k_4, \lambda_4), \tag{5}$$

FIG. 2. Feynman diagrams contributing to the $\gamma\gamma \rightarrow Y^{--}Y^{++}$ reaction.

where $\epsilon^{\mu}(k_1, \lambda_1)$, $\epsilon^{\nu}(k_2, \lambda_2)$ etc. represent the polarization four-vectors associated with the external particles. As a consequence of electromagnetic gauge invariance, the $\mathcal{M}_{\mu\nu\alpha\beta}$ tensorial amplitude obeys the following Ward identities:

$$k_1^{\mu}\mathcal{M}_{\mu\nu\alpha\beta} = k_2^{\nu}\mathcal{M}_{\mu\nu\alpha\beta} = 0. \quad (6)$$

It turns out to be that in the most general case, i.e. for an arbitrary κ parameter, the amplitude is characterized by six independent tensor structures which satisfy the gauge conditions. So, the tensorial amplitude can be written as follows:

$$\mathcal{M}_{\mu\nu\alpha\beta} = \sum_{i=1}^{6} f_i N^i_{\mu\nu\alpha\beta}, \quad (7)$$

where the $N^i_{\mu\nu\alpha\beta}$ are the tensor structures, which are given by

$$N^1_{\mu\nu\alpha\beta} = (1 + 3\kappa)\left(-\frac{\hat{s}}{2}g_{\mu\alpha}g_{\nu\beta} + k_{1\alpha}k_{2\mu}g_{\nu\beta}\right.$$
$$\left. - k_{1\alpha}k_{2\beta}g_{\mu\nu} + k_{2\beta}k_{1\nu}g_{\mu\alpha}\right), \quad (8)$$

$$N^2_{\mu\nu\alpha\beta} = (1 + 3\kappa)\left(-\frac{\hat{s}}{2}g_{\nu\alpha}g_{\mu\beta} + k_{2\alpha}k_{1\nu}g_{\mu\beta}\right.$$
$$\left. - k_{2\alpha}k_{1\beta}g_{\mu\nu} + k_{1\beta}k_{2\mu}g_{\nu\alpha}\right), \quad (9)$$

$$N^3_{\mu\nu\alpha\beta} = 4g_{\alpha\beta}\left(\frac{g_{\mu\nu}}{2f_1 f_2} + \hat{s}k_{3\mu}k_{3\nu} - \frac{k_{2\mu}k_{3\nu}}{f_1} - \frac{k_{3\mu}k_{1\nu}}{f_2}\right), \quad (10)$$

$$N^4_{\mu\nu\alpha\beta} = 2(1 + \kappa)\left[(k_{2\alpha}g_{\beta\nu} - k_{2\beta}g_{\alpha\nu})\left(\hat{s}k_{3\mu} - \frac{k_{2\mu}}{f_1}\right)\right.$$
$$\left. + (k_{1\alpha}g_{\mu\beta} - k_{1\beta}g_{\mu\alpha})\left(\hat{s}k_{3\nu} - \frac{k_{1\nu}}{f_2}\right)\right], \quad (11)$$

$$N^5_{\mu\nu\alpha\beta} = (1 - \kappa)(2f_1 k_{1\alpha}k_{3\mu} - g_{\mu\alpha})$$
$$\times [g_{\nu\beta} + 2f_1 k_{2\beta}(k_3 - k_1)_{\nu}], \quad (12)$$

$$N^6_{\mu\nu\alpha\beta} = (1 - \kappa)(2f_2 k_{2\alpha}k_{3\nu} - g_{\nu\alpha})$$
$$\times [g_{\mu\beta} + 2f_2 k_{1\beta}(k_3 - k_2)_{\mu}]. \quad (13)$$

In the above expressions, the f_i Lorentz scalars are given by

$$f_1 = \frac{1}{m_Y^2 - \hat{t}}, \qquad f_2 = \frac{1}{m_Y^2 - \hat{u}}, \quad (14)$$

$$f_3 = f_4 = f_1 f_2, \quad (15)$$

$$f_5 = \frac{1}{4m_Y^2 f_1}, \qquad f_6 = \frac{1}{4m_Y^2 f_2}. \quad (16)$$

Notice that the number of tensor structures reduces to four for a gauge bilepton without the presence of anomalous static electromagnetic properties ($\kappa = 1$).

The unpolarized cross section for the $\gamma\gamma \rightarrow Y^{--}Y^{++}$ subprocess is given by

$$\hat{\sigma}(\gamma\gamma \rightarrow Y^{--}Y^{++}) = \frac{1}{16\pi^2\hat{s}^2}\int_{\hat{t}_1}^{\hat{t}_2} d\hat{t}|\bar{\mathcal{M}}|^2, \quad (17)$$

where the integration limits are given by

$$\hat{t}_2(\hat{t}_1) = -\frac{\hat{s}}{4}\left(1 \pm \sqrt{1 - \frac{4m_Y^2}{\hat{s}}}\right). \quad (18)$$

After solving the integral, one obtains

$$\hat{\sigma}(\gamma\gamma \rightarrow Y^{--}Y^{++}) = \frac{\pi\alpha^2 Q_Y^4}{\hat{s}}F(x, \kappa), \quad (19)$$

where $x = 4m_Y^2/\hat{s}$ and

$$F(x, \kappa) = (-3(\kappa - 481)x^5 + (223\kappa - 1952)x^4$$
$$+ 3(1733\kappa + 1179)x^3 + (10175 - 9407\kappa)x^2$$
$$+ 4(8533\kappa - 2389)x - 2400(\kappa - 1))\mathcal{A}_1(x)$$
$$+ \left(\frac{24x^3 - 4(\kappa + 1)x^2 + (1 - \kappa)x - 22(\kappa - 1)}{8x}\right)$$
$$\times \mathcal{A}_2(x). \quad (20)$$

The $\mathcal{A}_i$ functions appearing in the above expression are given by

$$\mathcal{A}_1(x) = \frac{\sqrt{1 - x}}{48x^2(x^3 - 2x^2 - 7x + 24)}, \quad (21)$$

$$\mathcal{A}_2(x) = \log\left[\frac{4(1 + \sqrt{1 - x}) - x(x - 1)}{4(1 - \sqrt{1 - x}) - x(x - 1)}\right], \quad (22)$$

Notice that, as it could be expected, $F(1, \kappa) = 0$.

With the photons originating from Compton laser backscattering, the unpolarized cross section for the complete $e^+ e^- \rightarrow \gamma\gamma \rightarrow Y^{--}Y^{++}$ process is given by

$$\sigma(s) = \int_{2m_Y^2/\sqrt{s}}^{y_{max}} dz \frac{d\mathcal{L}_{\gamma\gamma}}{dz} \hat{\sigma}(\gamma\gamma \rightarrow Y^{--}Y^{++}), \quad (23)$$

where $\hat{s} = z^2 s$, with $\sqrt{s}(\sqrt{\hat{s}})$ the center of mass energies of the $e^+ e^- (\gamma\gamma)$ collisions, and $\frac{d\mathcal{L}_{\gamma\gamma}}{dz}$ is the photon luminosity, defined as

$$\frac{d\mathcal{L}_{\gamma\gamma}}{dz} = 2z \int_{z^2/y_{max}}^{y_{max}} \frac{dy}{y} f_{\gamma/e}(y) f_{\gamma/e}(z^2/y), \quad (24)$$

where the energy spectrum of the backscattered photon is given by [21]

$$f_{\gamma/e}(y) = \frac{1}{D(\chi)}\left[1 - y + \frac{1}{1 - y} - \frac{4y}{\chi(1 - y)} + \frac{4y^2}{\chi^2(1 - y)^2}\right], \quad (25)$$

with

$$D(\chi) = \left(1 - \frac{4}{\chi} - \frac{8}{\chi^2}\right)\log(1 + \chi) + \frac{1}{2} + \frac{8}{\chi} - \frac{1}{2(1 + \chi)^2}. \quad (26)$$

In this expression, $\chi = (4E_0\omega_0)/m_e^2$, where m_e and E_0 are the mass and energy of the electron, respectively; ω_0 is the laser-photon energy, and y represents the fraction of the energy of the incident electron carried by the backscattered photon. The optimum values for the y_{max} and χ parameters are $y_{max} \approx 0.83$ and $\chi = 2(1 + \sqrt{2})$. Notice that the x and z variables are related through $x = 4m_Y^2/sz^2$.

It has been customary to treat numerically the $\frac{d\mathcal{L}_{\gamma\gamma}}{dz}$ photon luminosity, but we prefer to solve it analytically. After solving this integral given through Eqs. (24)–(26), one obtains

$$\frac{d\mathcal{L}_{\gamma\gamma}}{dz} = \frac{4z}{D(\chi)^2(z^2 - 1)^4\chi^4}\left[g_0(z) + g_1(z)\log(y_{max})\right.$$
$$\left. + g_2(z)\log(z) + g_3(z)\log\left(\frac{z^2 - y_{max}}{y_{max} - 1}\right)\right], \quad (27)$$

where

$$g_0(z) = -16y_{max}(y_{max}^2 - z^2)(z^4 + \chi z^2(z^2 - 1))$$
$$+ 4\chi^2 y_{max}(y_{max}^2 - z^2)(z^6 - 3z^4 + 4z^2 - 2)$$
$$- 2\chi^4(y_{max} - 1)(z^2 - 1)^2(z^4 - y_{max}z^2(y_{max} + 1)$$
$$+ \chi^3), \quad (28)$$

$$g_1(z) = 2\chi^2(z^2 - 1)^3(\chi(2z^2 + \chi + 4) + 4), \quad (29)$$

$$g_2(z) = -8\chi^3 z^4(z^2 - 1)^2 + 16z^4(z^2 + 1)$$
$$+ 32\chi z^4(z^2 - 1) + 8\chi^2 z^2(z^4 - 3z^2 + 2)$$
$$+ \chi^4(z^4 - 3z^3 + 2)^2, \quad (30)$$

$$g_3(z) = -16z^4(z^2 + 1) - 32(z^2 - 1)$$
$$- \chi^4(z^2 - 1)^2(z^4 - 2z^2 + 2)$$
$$+ 4\chi^3(z^2 - 1)^2(z^4 - z^2 + 2)$$
$$- 8\chi^3(2z^6 - 6z^4 + 5z^2 - 1). \quad (31)$$

The total cross section $\sigma(s)$ cannot be expressed in closed form and will be numerically evaluated in the next section.

IV. RESULTS AND DISCUSSION

The next linear colliders $e^+ e^-$ in the TeV region, including its derivations γe and $\gamma\gamma$, will open up new opportunities in particle physics [22]. Although these colliders are intended to operate initially at a center of mass energy of a few hundreds of GeVs with a luminosity of the order of 10^{33} cm^{-2} s^{-1}, it is contemplated to increase the energy up to about 2000 GeV in subsequent stages. In particular, the $\gamma\gamma$ collisions offer the opportunity of accessing to physical information not available from $e^+ e^-$ colliders. Although the same type of particles can be produced in these colliders, it is important to stress that the reactions are different and thus complementary information can be obtained. One important feature of the $\gamma\gamma$ colliders is that the cross sections are much larger than in $e^+ e^-$ collisions. For instance, the cross section of W pair production in the $\gamma\gamma$ collision is almost 2 orders of magnitude higher than the W pair production in $e^+ e^-$ collisions. Another important difference between $e^+ e^-$ and $\gamma\gamma$ collisions is that, while the cross sections in the former decreases for increasing energies, those associated with the latter are almost constant. One disadvantage of a $\gamma\gamma$ collider is that its energy reaches approximately 80% of the parent $e^+ e^-$ collider. Thus, $e^+ e^-$ colliders operating in the region of a few TeVs will be necessary in order to investigate the production of new particles with masses in the sub-TeV region.

Having briefly discussed the main features of $\gamma\gamma$ colliders, we proceed to discuss our results. To begin with, it is convenient to comment on the bounds on the doubly charged vector bilepton mass. Currently, the most stringent bound arises from the conversion of muonium ($\mu^- e^+$) to antimuonium ($\mu^+ e^-$), which leads to the limit $m_Y > 1417 g_l$ GeV [23], where g_l is a model dependent constant coupling characterizing the $\bar{l}^c l Y^{++}$ vertex, which is expected to be smaller than 1. However, it has been argued that this bound can be evaded in a more general context
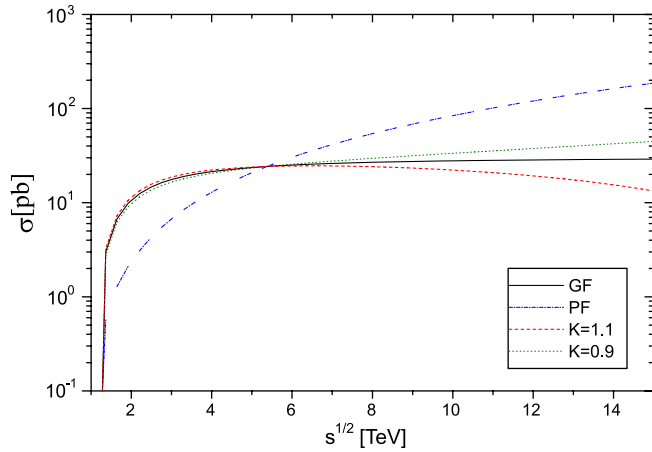
FIG. 3 (color online). The cross section for the $e^+e^- \rightarrow \gamma\gamma \rightarrow Y^{--}Y^{++}$ reaction as a function of the center of mass energy for $m_Y = 450$ GeV. Contributions of PF ($\kappa = 0$) and GF ($\kappa = 1$), including anomalous effects ($\kappa = 0.9$ and $\kappa = 1.1$), are shown.

since it relies on very restrictive assumptions [24]. Another strong limit, $m_Y > 1250g_l$ GeV, arises from fermion pair production and lepton flavor violating decays [25]. Recently, a more realistic constraint, $m_Y > 577g_l$, was derived from Bhabha scattering with CERN LEP data [26]. We would like to stress that all the above bounds are model dependent, and so the existence of lighter doubly charged vector bileptons is still allowed. We will present results for a bilepton with mass in the range $2m_W < m_Y < 10m_W$, with m_W the SM W gauge boson mass.

Before analyzing our results for some $\sqrt{s}$ energies of e^+e^- colliders, it is interesting to investigate the high-energy behavior of the cross section. In Fig. 3, we present the $\sigma(e^+e^- \rightarrow \gamma\gamma \rightarrow Y^{--}Y^{++})$ cross section as a function of $\sqrt{s}$ for both PF ($\kappa = 0$) and GF bileptons ($\kappa = 1$), including anomalous effects that represent deviations of 10% with respect to the renormalizable value of κ. As already mentioned, the former case defines vector electro-

dynamics, which, as it is well known, is not a predictive theory. The latter case corresponds to a $F_{\mu\nu}Y^{--\mu}Y^{++\nu}$ coupling induced by a Yang-Mills strength tensor $F_{\mu\nu}^a$. From this figure, it can be appreciated that the cross section associated with GF without anomalous contributions has a good high-energy behavior, as it tends to a constant value for increasing energies. As already mentioned, this essentially constant behavior of the cross section for the case of a GF is a peculiarity of $\gamma\gamma$ colliders. In contrast, in the case of PF, the corresponding cross section is ill behavior at high energies. As far as the anomalous effects are concerned, it can be appreciated that, for the values $m_Y = 450$ GeV and $\Delta\kappa = \pm 0.1$, the cross section is sensitive only for energies higher than about 1 order of magnitude than the bilepton mass. It can also be observed that, for increasing energies, the cross section decreases for $\kappa > 1$ and increases for $\kappa < 1$. These results suggest that an unmoderated growth of the cross section is expected in the range $0 \leq \kappa < 1$, reaching its highest ill behavior with the energy for a PF ($\kappa = 0$). These results agree with the well-known fact that only Yang-Mills theories ($\kappa = 1$) lead to well-behaved cross sections of binary processes involving massive vector bosons [20].

We now turn to discuss our results for some scenarios. We will analyze only the PF and GF cases, as they represent two extreme situations. We will present results for the cross section σ and the number of events N using an integrated luminosity of 10 fb^{-1} and energies of $\sqrt{s} = 0.5$, 1, 1.5, and 2 TeV. In Fig. 4, the number of events and the cross section are presented as functions of m_Y and for $\sqrt{s} = 0.5$ TeV. We can see that for a relatively light bilepton, with mass in the range $2m_W < m_Y < 200$ GeV, the cross section for a GF ranges between almost 29 and 0.55 pb, and it is approximately 5 times larger than that of the PF. With the luminosity considered, the number of events of GF bileptons ranges between 9×10^5 and 1.7×10^4. As it occurs with the cross sections, the number of events of GF and the number of events of PF differ in the
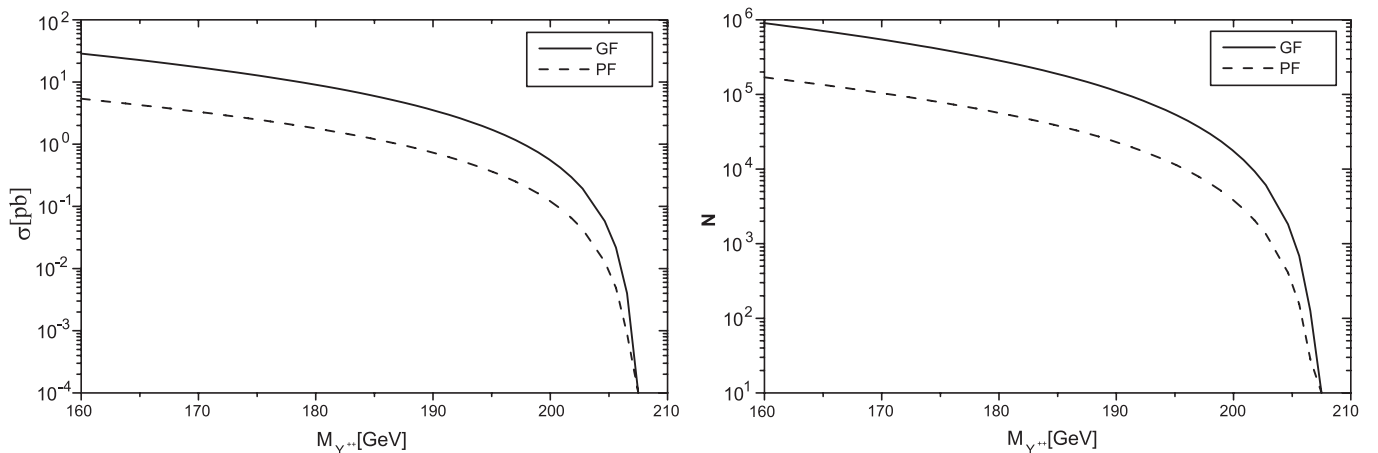

FIG. 4. The cross section and the number of events (N) as a function of m_Y for $\sqrt{s} = 0.5$ TeV.
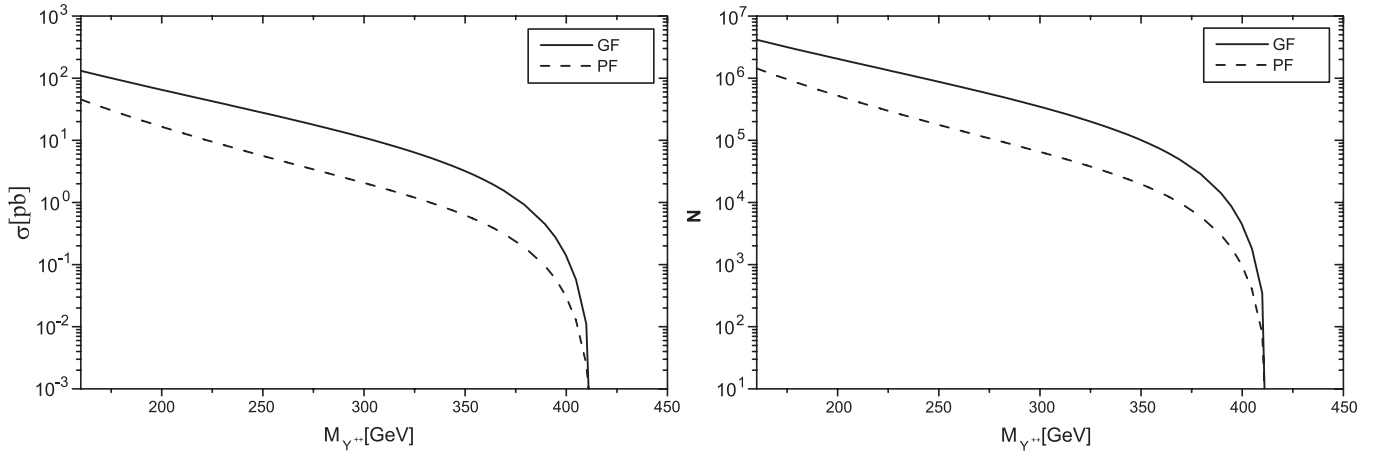
FIG. 5.   The same as Fig. 4, but now for $\sqrt{s} = 1$ TeV.
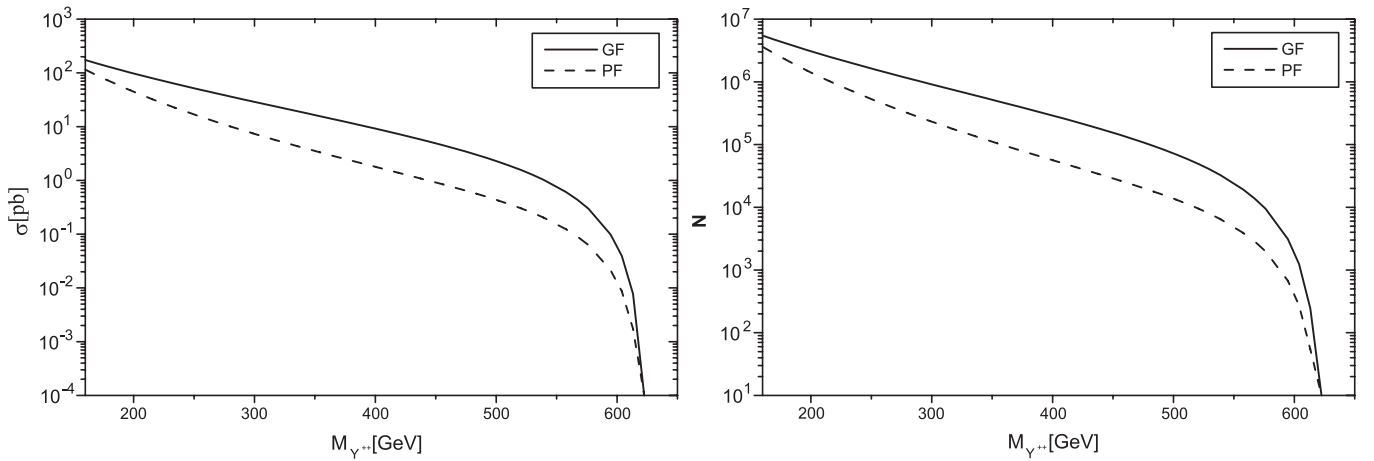

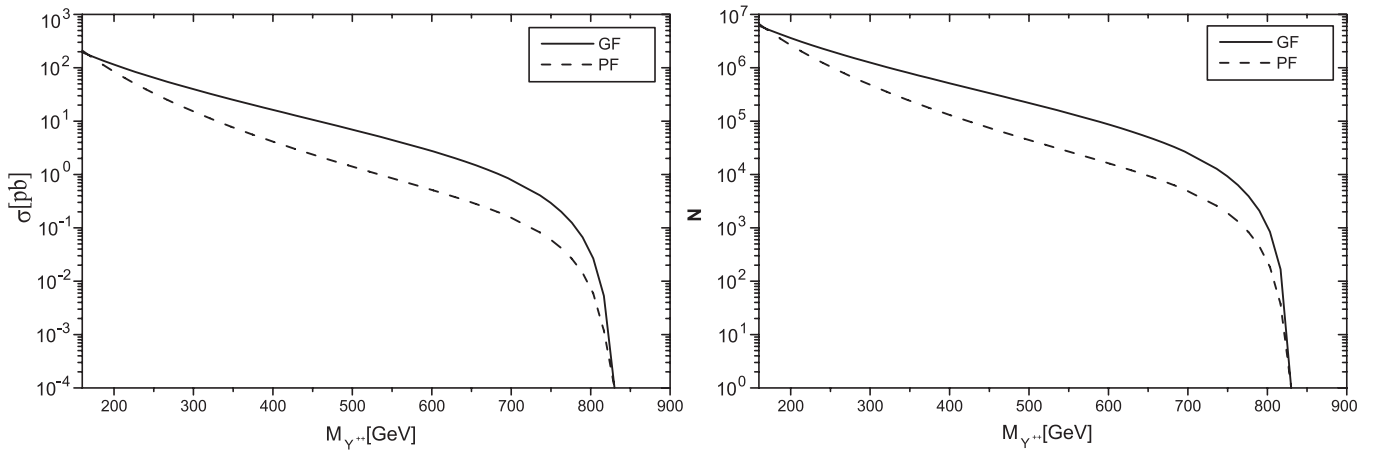FIG. 6.   The same as Fig. 4, but now for $\sqrt{s} = 1.5$ TeV.

FIG. 7.   The same as Fig. 4, but now for $\sqrt{s} = 2$ TeV.

same proportion. Indeed, the $\sigma_{GF}/\sigma_{NGF} = N_{GF}/N_{NGF} = R < 1$ ratios are true for any energy, as it can be observed from Figs. 4–7. It is also evident from these figures that R decreases for increasing energies, as σ_{NGF} increases whereas at the same time σ_{GF} remains essentially constant. Indeed, in the range $0.5 < \sqrt{s} < 2$ TeV, R is always smaller than 1, as it can be appreciated from Fig. 3. In the following, we will concentrate on the number of events and only for the case of GF bileptons. Thus, from Fig. 5, we can see that N ranges between 4×10^6 and 10^5 for $\sqrt{s} = 1$ TeV and $2m_W < m_Y < 350$ GeV. On the other hand, from Fig. 6, we can appreciate that, for $\sqrt{s} = 1.5$ TeV, N goes from 5.5×10^6 for $m_Y = 2m_W$ to 7.2×10^4 for $m_Y = 500$ GeV. Finally, it is found that, for $\sqrt{s} = 2$ TeV, N goes from 6.2×10^6 for $m_Y = 2m_W$ to 10^3 for $m_Y = 800$ GeV.

It is interesting to compare our results with the case of W pair production. Using the same integrated luminosity for the convoluted cross section, the number of events is approximately 10^6, 1.5×10^6, 1.7×10^6, and 1.8×10^6 for energies of 0.5, 1, 1.5, and 2 TeV, respectively. The number of events estimated in the literature for a nonconvoluted cross section, at energies above 200 GeV and for an integrated luminosity of 100 fb^{-1}, is about 8×10^6 [22].

V. CONCLUSIONS

A $\gamma\gamma$ collider is the ideal place to study the production of pairs of new charged particles and their properties, as the cross sections are large and model independent at the tree level. In this work, we have studied the production of pairs of doubly charged vector bileptons, whose decay modes $Y^{\pm\pm} \to 2l^{\pm}$ will provide a spectacular signature, since it is almost free of SM background. The unpolarized cross section for the $\gamma\gamma \to Y^{--}Y^{++}$ subprocess was analyti-

cally derived and then convoluted to predict the cross section and the number of events of the complete $e^+e^- \to \gamma\gamma \to Y^{--}Y^{++}$ process. Our results are valid for an arbitrarily charged vector boson that includes anomalous couplings characterized by the dimension-four operator $ie\kappa F_{\mu\nu}Y^{--\mu}Y^{++\nu}$, with κ a real arbitrary parameter. The renormalizable case ($\kappa = 1$), which corresponds to a gauge bilepton, as well as the possibility of a matter vector ($\kappa = 0$), which corresponds to vector electrodynamics, were analyzed. The possibility of a gauge bilepton with anomalous interactions was studied also. Two specific values were considered, namely, $\kappa = 0.9$ and $\kappa = 1.1$. It was shown that, as it is well known, the cross section has a high-energy well behavior only for the case $\kappa = 1$, and it is essentially constant for increasing energies. On the other hand, for the case of a nonrenormalizable Lagrangian, it was found that, for increasing energies, the cross section increases for values of κ ranging from 0 to 1, but decreases for $\kappa > 1$. The worst of all of the behaviors is found for $\kappa = 0$. The situation is reversed when the cross section is analyzed as a function of the bilepton mass m_Y. In this case, for a given energy, the largest and smallest number of events is found for $\kappa = 1$ and $\kappa = 0$, respectively. Our conclusion is that this class of exotic particles can be detected still if they are as heavy as about $10m_W$, as the number of events is relatively large, of about 10^3, and their signature is spectacular.

[1] For a review, see F. Cuypers and S. Davidson, Eur. Phys. J. C **2**, 503 (1998).

[2] J. C. Pati and A. Salam, Phys. Rev. D **10**, 275 (1974); R. N. Mohapatra and J. C. Pati, Phys. Rev. D **11**, 566 (1975); **11**, 2558 (1975); G. Senjanovic and R. N. Mohapatra, Phys. Rev. D **12**, 1502 (1975); R. N. Mohapatra and G. Senjanovic, Phys. Rev. D **23**, 165 (1981).

[3] For a review, see W. Buchmuller, Acta Phys. Austriaca Suppl. **27**, 517 (1985).

[4] For a review see, for instance, E. Fahri and L. Susskind, Phys. Rep. **74**, 277 (1981).

[5] P. H. Frampton and B.-H. Lee, Phys. Rev. Lett. **64**, 619 (1990); P. B. Pal, Phys. Rev. D **43**, 236 (1991).

[6] P. H. Frampton, Phys. Rev. Lett. **69**, 2889 (1992); F. Pisano and V. Pleitez, Phys. Rev. D **46**, 410 (1992).

[7] P. H. Frampton, Mod. Phys. Lett. A **7**, 2017 (1992); Jonathan L. Feng, Int. J. Mod. Phys. A **15**, 2355 (2000).

[8] J. F. Gunion, Int. J. Mod. Phys. A **13**, 2277 (1998).

[9] P. H. Frampton and D. Ng, Phys. Rev. D **45**, 4240 (1992); T. G. Rizzo, Phys. Rev. D **46**, 910 (1992); F. Cuypers and M. Raidal, Nucl. Phys. **B501**, 3 (1997); M. Raidal, Phys. Rev. D **57**, 2013 (1998); P. H. Frampton, Int. J. Mod. Phys. A **13**, 2345 (1998); P. H. Frampton and A. Rasin, Phys. Lett. B **482**, 129 (2000); Paul H. Frampton, Int. J. Mod. Phys. A **15**, 2455 (2000).

[10] See, for instance, G. Tavares-Velasco and J. J. Toscano, Phys. Rev. D **65**, 013005 (2002).

[11] B. Bion, T. Grégoire, D. London, L. Marleau, and H. Nadeau, Phys. Rev. D **59**, 075006 (1999).

[12] J. Agrawal, P. H. Frampton, and D. Ng, Nucl. Phys. **B386**, 267 (1992); P. H. Frampton and B. C. Rasco, Phys. Rev. Lett. **75**, 1899 (1995).

[13] Hoang Ngoc Long and Dang Van Soa, Nucl. Phys. **B601**, 361 (2001).

[14] Dang Van Soa, Takeo Inami, and Hoang Ngoc Long, Eur. Phys. J. C **34**, 285 (2004).

[15] P. H. Frampton and X. Guan, Mod. Phys. Lett. A **13**, 2621 (1998).

[16] N. Leporé, B. Thorndyke, H. Nadeau, and D. London, Phys. Rev. D **50**, 2031 (1994).

[17] For a comprehensive discussion on the static electromagnetic properties of arbitrarily charged vector boson, see G. Tavares-Velasco and J. J. Toscano, J. Phys. G **30**, 1299 (2004).

[18] See, for instance, R. Johnson and B.-L. Young, Phys. Rev. D **42**, 3855 (1990); C. T. Hill and D. C. Kennedy, Phys. Rev. **47**, 2940 (1993); C. X. Yue, G. R. Lu, and L. D. Wan, J. Phys. G **21**, 595 (1995).

[19] For a review, see J. Ellison and J. Wudka, Annu. Rev. Nucl. Part. Sci. **48**, 33 (1998).

[20] S. Weinberg, Phys. Rev. Lett. **27**, 1688 (1971); J. Schechter and Y. Ueda, Phys. Rev. D **7**, 3119 (1973); J. M. Cornwall, D. N. Levin, and G. Tiktopoulos, Phys. Rev. D **10**, 1145 (1974).

[21] V. Telnov, Nucl. Instrum. Methods Phys. Res., Sect. A **294**, 72 (1990).

[22] See, for instance, E. Boos *et al.*, Nucl. Instrum. Methods Phys. Res., Sect. A **472**, 100 (2001), and references therein.

[23] L. Willmann *et al.*, Phys. Rev. Lett. **82**, 49 (1999).

[24] V. Pleitez, Phys. Rev. D **61**, 057903 (2000); P. Das and P. Jain, *ibid.* **62**, 075001 (2000); P. H. Frampton and A. Rasin, Phys. Lett. B **482**, 129 (2000).

[25] M. B. Tully and G. C. Joshi, Phys. Lett. B **466**, 333 (1999).

[26] S. Atağ and K. O. Ozansoy, Phys. Rev. D **68**, 093008 (2003).